Physics Letters B 670 (2009) 313–320

Contents lists available at ScienceDirect

Physics Letters B

www.elsevier.com/locate/physletb

Dilepton mass spectra in $p+p$ collisions at $\sqrt{s}=200$ GeV and the contribution from open charm

PHENIX Collaboration

A. Adare [h], S. Afanasiev [v], C. Aidala [i], N.N. Ajitanand [av], Y. Akiba [ap,aq], H. Al-Bataineh [ak], J. Alexander [av], K. Aoki [aa,ap], L. Aphecetche [ax], R. Armendariz [ak], S.H. Aronson [c], J. Asai [aq], E.T. Atomssa [ab], R. Averbeck [aw], T.C. Awes [al], B. Azmoun [c], V. Babintsev [r], G. Baksay [n], L. Baksay [n], A. Baldisseri [k], K.N. Barish [d], P.D. Barnes [ad], B. Bassalleck [aj], S. Bathe [d], S. Batsouli [al], V. Baublis [ao], A. Bazilevsky [c], S. Belikov [c,1], R. Bennett [aw], Y. Berdnikov [as], A.A. Bickley [h], J.G. Boissevain [ad], H. Borel [k], K. Boyle [aw], M.L. Brooks [ad], H. Buesching [c], V. Bumazhnov [r], G. Bunce [c,aq], S. Butsyk [ad,aw], S. Campbell [aw], B.S. Chang [be], J.-L. Charvet [k], S. Chernichenko [r], J. Chiba [w], C.Y. Chi [i], M. Chiu [s], I.J. Choi [be], T. Chujo [bb], P. Chung [av], A. Churyn [r], V. Cianciolo [al], C.R. Cleven [p], B.A. Cole [i], M.P. Comets [am], P. Constantin [ad], M. Csanád [m], T. Csörgő [y], T. Dahms [aw], K. Das [o], G. David [c], M.B. Deaton [a], K. Dehmelt [n], H. Delagrange [ax], A. Denisov [r], D. d'Enterria [i], A. Deshpande [aq,aw], E.J. Desmond [c], O. Dietzsch [at], A. Dion [aw], M. Donadelli [at], O. Drapier [ab], A. Drees [aw], A.K. Dubey [bd], A. Durum [r], V. Dzhordzhadze [d], Y.V. Efremenko [al], J. Egdemir [aw], F. Ellinghaus [h], W.S. Emam [d], A. Enokizono [ac], H. En'yo [ap,aq], S. Esumi [ba], K.O. Eyser [d], D.E. Fields [aj,aq], M. Finger [e,v], M. Finger Jr. [e,v], F. Fleuret [ab], S.L. Fokin [z], Z. Fraenkel [bd,1], J.E. Frantz [aw], A. Franz [c], A.D. Frawley [o], K. Fujiwara [ap], Y. Fukao [aa,ap], T. Fusayasu [ai], S. Gadrat [ae], I. Garishvili [ay], A. Glenn [h], H. Gong [aw], M. Gonin [ab], J. Gosset [k], Y. Goto [ap,aq], R. Granier de Cassagnac [ab], N. Grau [u], S.V. Greene [bb], M. Grosse Perdekamp [s,aq], T. Gunji [g], H.-Å. Gustafsson [af], T. Hachiya [q], A. Hadj Henni [ax], C. Haegemann [aj], J.S. Haggerty [c], H. Hamagaki [g], R. Han [an], H. Harada [q], E.P. Hartouni [ac], K. Haruna [q], E. Haslum [af], R. Hayano [g], M. Heffner [ac], T.K. Hemmick [aw], T. Hester [d], X. He [p], H. Hiejima [s], J.C. Hill [u], R. Hobbs [aj], M. Hohlmann [n], W. Holzmann [av], K. Homma [q], B. Hong [y], T. Horaguchi [ap,az], D. Hornback [ay], T. Ichihara [ap,aq], K. Imai [aa,ap], M. Inaba [ba], Y. Inoue [ar,ap], D. Isenhower [a], L. Isenhower [a], M. Ishihara [ap], T. Isobe [g], M. Issah [av], A. Isupov [v], B.V. Jacak [aw,2], J. Jia [i], J. Jin [i], O. Jinnouchi [aq], B.M. Johnson [c,*], K.S. Joo [ah], D. Jouan [am], F. Kajihara [g], S. Kametani [g,bc], N. Kamihara [ap], J. Kamin [aw], M. Kaneta [aq], J.H. Kang [be], H. Kanou [ap,az], D. Kawall [aq], A.V. Kazantsev [z], A. Khanzadeev [ao], J. Kikuchi [bc], D.H. Kim [ah], D.J. Kim [be], E. Kim [au], E. Kinney [h], A. Kiss [m], E. Kistenev [c], A. Kiyomichi [ap], J. Klay [ac], C. Klein-Boesing [ag], L. Kochenda [ao], V. Kochetkov [r], B. Komkov [ao], M. Konno [ba], D. Kotchetkov [d], A. Kozlov [bd], A. Král [j], A. Kravitz [i], J. Kubart [e,t], G.J. Kunde [ad], N. Kurihara [g], K. Kurita [ar,ap], M.J. Kweon [y], Y. Kwon [ay,be], G.S. Kyle [ak], R. Lacey [av], Y.-S. Lai [i], J.G. Lajoie [u], A. Lebedev [u], D.M. Lee [ad], M.K. Lee [be], T. Lee [au], M.J. Leitch [ad], M.A.L. Leite [at], B. Lenzi [at], T. Liška [j], A. Litvinenko [v], M.X. Liu [ad], X. Li [f], B. Love [bb], D. Lynch [c], C.F. Maguire [bb], Y.I. Makdisi [c], A. Malakhov [v], M.D. Malik [aj], V.I. Manko [z], Y. Mao [an,ap], L. Mašek [e,t], H. Masui [ba], F. Matathias [i], M. McCumber [aw], P.L. McGaughey [ad], Y. Miake [ba], P. Mikeš [e,t], K. Miki [ba], T.E. Miller [bb], A. Milov [aw], S. Mioduszewski [c], M. Mishra [b], J.T. Mitchell [c], M. Mitrovski [av], A. Morreale [d], D.P. Morrison [c], T.V. Moukhanova [z], D. Mukhopadhyay [bb], J. Murata [ar,ap], S. Nagamiya [w], Y. Nagata [ba], J.L. Nagle [h], M. Naglis [bd], I. Nakagawa [ap,aq], Y. Nakamiya [q], T. Nakamura [q], K. Nakano [ap,az], J. Newby [ac], M. Nguyen [aw], B.E. Norman [ad], A.S. Nyanin [z], E. O'Brien [c], S.X. Oda [g], C.A. Ogilvie [u], H. Ohnishi [ap], H. Okada [aa,ap], K. Okada [aq], M. Oka [ba], O.O. Omiwade [a], A. Oskarsson [af], M. Ouchida [q], K. Ozawa [g], R. Pak [c], D. Pal [bb], A.P.T. Palounek [ad], V. Pantuev [aw], V. Papavassiliou [ak], J. Park [au], W.J. Park [y], S.F. Pate [ak], H. Pei [u], J.-C. Peng [s], H. Pereira [k], V. Peresedov [v], D.Yu. Peressounko [z], C. Pinkenburg [c], M.L. Purschke [c], A.K. Purwar [ad], H. Qu [p], J. Rak [aj], A. Rakotozafindrabe [ab], I. Ravinovich [bd], K.F. Read [al,ay], S. Rembeczki [n], M. Reuter [aw], K. Reygers [ag], V. Riabov [ao], Y. Riabov [ao], G. Roche [ae], A. Romana [ab,1], M. Rosati [u], S.S.E. Rosendahl [af], P. Rosnet [ae], P. Rukoyatkin [v], V.L. Rykov [ap], B. Sahlmueller [ag], N. Saito [aa,ap,aq], T. Sakaguchi [c], S. Sakai [ba], H. Sakata [q], V. Samsonov [ao], S. Sato [w], S. Sawada [w], J. Seele [h], R. Seidl [s], V. Semenov [r], R. Seto [d], D. Sharma [bd], I. Shein [r], A. Shevel [ao,av], T.-A. Shibata [ap,az], K. Shigaki [q], M. Shimomura [ba], K. Shoji [aa,ap], A. Sickles [aw], C.L. Silva [at], D. Silvermyr [al], C. Silvestre [k], K.S. Sim [y], C.P. Singh [b], V. Singh [b], S. Skutnik [u], M. Slunečka [e,v], A. Soldatov [r],

0370-2693/$ – see front matter
doi:10.1016/j.physletb.2008.10.064

R.A. Soltz [ac], W.E. Sondheim [ad], S.P. Sorensen [ay], I.V. Sourikova [c], F. Staley [k], P.W. Stankus [al], E. Stenlund [af], M. Stepanov [ak], A. Ster [x], S.P. Stoll [c], T. Sugitate [q], C. Suire [am], J. Sziklai [x], T. Tabaru [aq], S. Takagi [ba], E.M. Takagui [at], A. Taketani [ap,aq], Y. Tanaka [ai], K. Tanida [ap,aq], M.J. Tannenbaum [c], A. Taranenko [av], P. Tarján [l], T.L. Thomas [aj], M. Togawa [aa,ap], A. Toia [aw], J. Tojo [ap], L. Tomášek [t], H. Torii [ap], R.S. Towell [a], V.-N. Tram [ab], I. Tserruya [bd], Y. Tsuchimoto [q], C. Vale [u], H. Valle [bb], H.W. van Hecke [ad], J. Velkoška [bb], R. Vertesi [l], A.A. Vinogradov [z], M. Virius [j], V. Vrba [t], E. Vznuzdaev [ao], M. Wagner [aa,ap], D. Walker [aw], X.R. Wang [ak], Y. Watanabe [ap,aq], J. Wessels [ag], S.N. White [c], D. Winter [i], C.L. Woody [c], M. Wysocki [h], W. Xie [aq], Y.L. Yamaguchi [bc], A. Yanovich [r], Z. Yasin [d], J. Ying [p], S. Yokkaichi [ap,aq], G.R. Young [al], I. Younus [aj], I.E. Yushmanov [z], W.A. Zajc [i], O. Zaudtke [ag], C. Zhang [al], S. Zhou [f], J. Zimányi [x,1], L. Zolin [v]

[a] *Abilene Christian University, Abilene, TX 79699, USA*
[b] *Department of Physics, Banaras Hindu University, Varanasi 221005, India*
[c] *Brookhaven National Laboratory, Upton, NY 11973-5000, USA*
[d] *University of California—Riverside, Riverside, CA 92521, USA*
[e] *Charles University, Ovocný trh 5, Praha 1, 116 36, Prague, Czech Republic*
[f] *China Institute of Atomic Energy (CIAE), Beijing, People's Republic of China*
[g] *Center for Nuclear Study, Graduate School of Science, University of Tokyo, 7-3-1 Hongo, Bunkyo, Tokyo 113-0033, Japan*
[h] *University of Colorado, Boulder, CO 80309, USA*
[i] *Columbia University, New York, NY 10027, and Nevis Laboratories, Irvington, NY 10533, USA*
[j] *Czech Technical University, Zikova 4, 166 36 Prague 6, Czech Republic*
[k] *Dapnia, CEA Saclay, F-91191, Gif-sur-Yvette, France*
[l] *Debrecen University, H-4010 Debrecen, Egyetem tér 1, Hungary*
[m] *ELTE, Eötvös Loránd University, H-1117 Budapest, Pázmány P.s. 1/A, Hungary*
[n] *Florida Institute of Technology, Melbourne, FL 32901, USA*
[o] *Florida State University, Tallahassee, FL 32306, USA*
[p] *Georgia State University, Atlanta, GA 30303, USA*
[q] *Hiroshima University, Kagamiyama, Higashi-Hiroshima 739-8526, Japan*
[r] *IHEP Protvino, State Research Center of Russian Federation, Institute for High Energy Physics, Protvino 142281, Russia*
[s] *University of Illinois at Urbana-Champaign, Urbana, IL 61801, USA*
[t] *Institute of Physics, Academy of Sciences of the Czech Republic, Na Slovance 2, 182 21 Prague 8, Czech Republic*
[u] *Iowa State University, Ames, IA 50011, USA*
[v] *Joint Institute for Nuclear Research, 141980 Dubna, Moscow Region, Russia*
[w] *KEK, High Energy Accelerator Research Organization, Tsukuba, Ibaraki 305-0801, Japan*
[x] *KFKI Research Institute for Particle and Nuclear Physics of the Hungarian Academy of Sciences (MTA KFKI RMKI), H-1525 Budapest 114, PO Box 49, Budapest, Hungary*
[y] *Korea University, Seoul 136-701, Republic of Korea*
[z] *Russian Research Center "Kurchatov Institute", Moscow, Russia*
[aa] *Kyoto University, Kyoto 606-8502, Japan*
[ab] *Laboratoire Leprince-Ringuet, Ecole Polytechnique, CNRS-IN2P3, Route de Saclay, F-91128 Palaiseau, France*
[ac] *Lawrence Livermore National Laboratory, Livermore, CA 94550, USA*
[ad] *Los Alamos National Laboratory, Los Alamos, NM 87545, USA*
[ae] *LPC, Université Blaise Pascal, CNRS-IN2P3, Clermont-Fd, 63177 Aubiere Cedex, France*
[af] *Department of Physics, Lund University, Box 118, SE-221 00 Lund, Sweden*
[ag] *Institut für Kernphysik, University of Muenster, D-48149 Muenster, Germany*
[ah] *Myongji University, Yongin, Kyonggido 449-728, Republic of Korea*
[ai] *Nagasaki Institute of Applied Science, Nagasaki-shi, Nagasaki 851-0193, Japan*
[aj] *University of New Mexico, Albuquerque, NM 87131, USA*
[ak] *New Mexico State University, Las Cruces, NM 88003, USA*
[al] *Oak Ridge National Laboratory, Oak Ridge, TN 37831, USA*
[am] *IPN-Orsay, Universite Paris Sud, CNRS-IN2P3, BP1, F-91406 Orsay, France*
[an] *Peking University, Beijing, People's Republic of China*
[ao] *PNPI, Petersburg Nuclear Physics Institute, Gatchina, Leningrad Region 188300, Russia*
[ap] *RIKEN, The Institute of Physical and Chemical Research, Wako, Saitama 351-0198, Japan*
[aq] *RIKEN BNL Research Center, Brookhaven National Laboratory, Upton, NY 11973-5000, USA*
[ar] *Physics Department, Rikkyo University, 3-34-1 Nishi-Ikebukuro, Toshima, Tokyo 171-8501, Japan*
[as] *Saint Petersburg State Polytechnic University, St. Petersburg, Russia*
[at] *Universidade de São Paulo, Instituto de Física, Caixa Postal 66318, São Paulo CEP05315-970, Brazil*
[au] *System Electronics Laboratory, Seoul National University, Seoul, Republic of Korea*
[av] *Chemistry Department, Stony Brook University, Stony Brook, SUNY, NY 11794-3400, USA*
[aw] *Department of Physics and Astronomy, Stony Brook University, SUNY, Stony Brook, NY 11794, USA*
[ax] *SUBATECH (Ecole des Mines de Nantes, CNRS-IN2P3, Université de Nantes), BP 20722-44307, Nantes, France*
[ay] *University of Tennessee, Knoxville, TN 37996, USA*
[az] *Department of Physics, Tokyo Institute of Technology, Oh-okayama, Meguro, Tokyo 152-8551, Japan*
[ba] *Institute of Physics, University of Tsukuba, Tsukuba, Ibaraki 305, Japan*
[bb] *Vanderbilt University, Nashville, TN 37235, USA*
[bc] *Waseda University, Advanced Research Institute for Science and Engineering, 17 Kikui-cho, Shinjuku-ku, Tokyo 162-0044, Japan*
[bd] *Weizmann Institute, Rehovot 76100, Israel*
[be] *Yonsei University, IPAP, Seoul 120-749, Republic of Korea*

ARTICLE INFO

Article history:
Received 5 February 2008
Received in revised form 30 October 2008
Accepted 31 October 2008
Available online 11 November 2008

ABSTRACT

PHENIX has measured the electron–positron pair mass spectrum from 0 to 8 GeV/c^2 in $p+p$ collisions at $\sqrt{s}=200$ GeV. The contributions from light meson decays to e^+e^- pairs have been determined based on measurements of hadron production cross sections by PHENIX. Within the systematic uncertainty of $\sim 20\%$ they account for all e^+e^- pairs in the mass region below ~ 1 GeV/c^2. The e^+e^- pair yield

Editor: V. Metag

remaining after subtracting these contributions is dominated by semileptonic decays of charmed hadrons correlated through flavor conservation. Using the spectral shape predicted by PYTHIA, we estimate the charm production cross section to be $544 \pm 39(\text{stat}) \pm 142(\text{syst}) \pm 200(\text{model})$ μb, which is consistent with QCD calculations and measurements of single leptons by PHENIX.

Because of the large mass of the charm quark, approximately 1.3 GeV/c^2, it is commonly expected that the charm production cross section can be calculated in quantum chromo-dynamics (QCD) using perturbative methods (pQCD). Comparing such calculations with experimental data serves as a test of pQCD and helps to quantify the importance of higher order terms. Perturbative calculations suggest that charm production at RHIC energies results primarily from gluon fusion, so charm can probe gluonic interactions in the matter formed in heavy ion collisions at RHIC [1]. Medium modifications of heavy quark production and the suppression of bound charmonium states like the J/ψ have received considerable attention and are thought to be keys to better understanding properties of strongly interacting matter. Experiments at RHIC with polarized proton beams will allow the measurement of spin asymmetries in charm production, which gives access to the spin contribution of the gluons to the proton in a new channel [2].

To date, charm production has been calculated in next-to-leading-order (NLO) and fixed-order plus next-to-leading-log approximations (FONLL) [3]. These calculations are consistent with the measured D meson cross sections in 1.96 TeV $p\bar{p}$ collisions published by CDF [4] as well as with single lepton measurements, electrons [5] and muons [6], in 200 GeV $p+p$ collisions from PHENIX. However, the theoretical uncertainties are considerable, at least a factor of two [3] or even larger [7], and the data prefer larger cross sections within these uncertainties.[3] In this Letter we present a different method to determine the charm cross section using electron–positron pairs measured with PHENIX during the RHIC $p+p$ run in 2005.

Electrons are measured in the two PHENIX central arm spectrometers [10], which each cover $|\eta| \leqslant 0.35$ in pseudo-rapidity and $\Delta\phi = \pi/2$ in azimuth in a nearly back-to-back configuration. For charged particles drift chambers (DC) measure the deflection angles in a magnetic field to determine their momenta. Ring imaging Cherenkov counters (RICH) as well as electromagnetic calorimeters (EMCal) distinguish electrons from other particles. The electron analysis is described in detail in [5].

Two data sets are used in the analysis. A reference sample of events was selected with a minimum bias interaction trigger (MB) that was based on beam–beam counters (BBC). The BBC trigger cross section is 23.0 ± 2.2 mb or $55 \pm 5\%$ of the inelastic $p+p$ cross section. Simulations, and data collected without requiring the BBC trigger, indicate that the triggered events include $79 \pm 2\%$ of events with particles in the central arm acceptance. This number coincides with the fraction of non-diffractive events triggered by the BBC from which we conclude that for non-diffractive collisions the BBC trigger can have only little bias towards events with particles produced in the central arms. The bulk of the data sample was recorded requiring a coincidence of the BBC trigger with a single electron trigger (ERT) that matches hits in the RICH to 2×2 trigger tiles in the EMCal with a minimum energy of 400 MeV. In the active area the ERT trigger has a very high efficiency for electrons; around 500 MeV it reaches approximately 50% and then saturates around 1 GeV close to 100%. After applying an interaction-vertex cut of ±30 cm the total integrated luminosities were 43 nb^{-1} and 2.25 pb^{-1} for the MB and ERT trigger, respectively.

All electrons and positrons with $p_T > 200$ MeV/c are combined into like- and unlike-sign pairs. For each pair we check that at least one of the tracks was registered by the ERT trigger. The event is rejected if the two tracks of the pair overlap in any of the detectors; this cut removes 2% of the e^+e^- pairs. This cut is necessary to assure that the combinatorial pair background is reproduced from mixed events. Pairs originating from photon conversions in the detector material are removed by a cut on the orientation of the opening angle of the pairs with respect to the magnetic field; this cut removes 98% of the pairs from photon conversions [11]. Fig. 1 shows the raw yields as a function of pair mass for both like- and unlike-sign pairs. The unlike-sign spectrum measures the signal from hadron decays and open charm plus background, while the like-sign spectrum measures only the background. The PHENIX central arms accept equal number of electrons and positrons, however, because of the two-arm geometry and the magnetic field, the acceptance for electrons and positrons covers a different range in azimuthal angle. Therefore the shape of the mass distribution is different for like- and unlike-sign pairs.

We have developed two independent methods to subtract the background. In the first method we decompose the background into two components: a combinatorial background made of uncorrelated pairs and a background of correlated pairs. The combinatorial background is determined from mixed events using the procedure described in more detail in [11,12] and in Appendix A of [13]. The mixed events are generated from the MB sample. For each pair we check that at least one of the two partners fulfill the ERT trigger condition. The mass distribution for the like-sign mixed event background does not have the same shape as the measured distribution, which indicates the presence of additional correlated background in the data. This can be studied in more detail investigating the pair distributions in mass versus transverse momentum. The biggest differences in shape are at low mass and large p_T as well as at low p_T and large mass, where the data show more yield than the mixed events. We therefore use a region, roughly corresponding to a mass of 300 MeV/c^2, p_T above 400 MeV/c and a transverse mass $m_T = \sqrt{m^2 + (p_T/c)^2}$ below 1.2 GeV/c^2, to normalize the mixed event background to the data.[4] In this region also the shape of the mass distributions are very similar. After normalizing the like-sign mass distribution from mixed events we determine the number of uncorrelated like-sign background pairs N_{++} and N_{--} by integrating the distributions. The normalization of the uncorrelated unlike-sign mixed event background is then given by $2\sqrt{N_{++}N_{--}}$.

The mixed event backgrounds as well as the distributions after subtraction are also shown in Fig. 1. The remaining pairs, like and unlike, are considered correlated pairs, where the like-sign distribution only contains correlated background pairs while the unlike contains also the signal. The correlated background pairs

* Corresponding author.
E-mail addresses: jacak@skipper.physics.sunysb.edu (B.V. Jacak), brant@bnl.gov (B.M. Johnson).

[1] Deceased.

[2] PHENIX Spokesperson.

[3] The STAR Collaboration reports an even larger cross section [8,9], which is about a factor of 2–3 above of what can be accommodated in pQCD calculations.

[4] The exact region used for the normalization is given by the following four conditions $m > 300$ MeV/c^2, $m_T < 1.2$ MeV/c^2, $p_T/c - 1.5m \leqslant 200$ MeV/c^2, and $p_T/c - 0.75m \geqslant -150$ MeV/c^2.

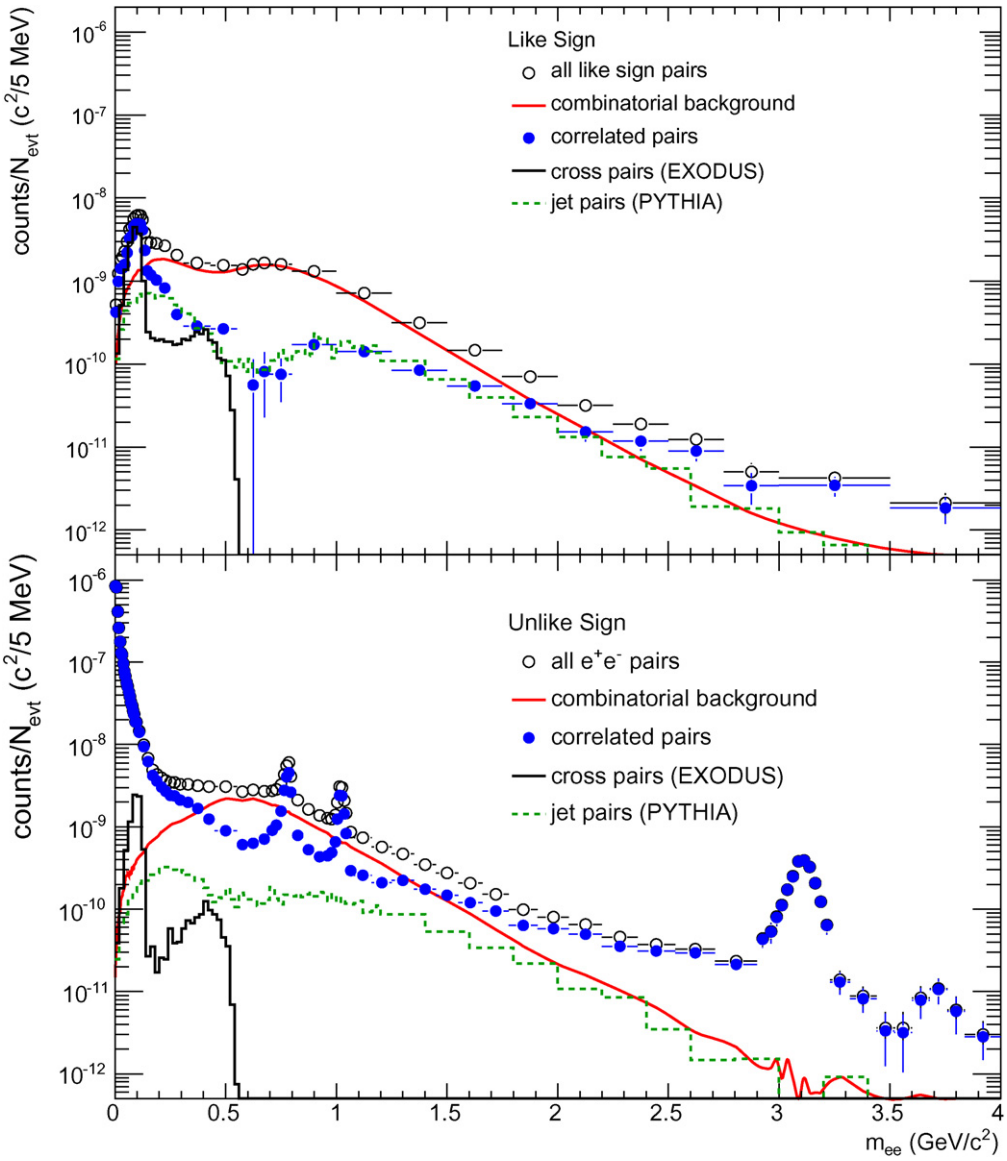

Fig. 1. Raw dielectron spectra. The top panel shows like-sign pairs as measured in the experiment, the combinatorial background from mixed events, the correlated pair background obtained by subtracting the combinatorial background, and the individual contributions from cross and jet pairs to the correlated background (see text). The bottom panel shows the same distributions for unlike-sign pairs.

stem from two sources. "Cross pairs" result from decays of single π^0 or η mesons with two electron pairs in the final state, such as double Dalitz decays, Dalitz decays plus conversion of the accompanying photon, and $\gamma\gamma$ decays where both photons convert. These pairs have a mass lower than the η mass of 548 MeV/c^2. Cross pairs were simulated using our hadron decay generator EXODUS including the PHENIX acceptance.[5] "Jet pairs" are produced by two independent hadron decays yielding electron pairs, either within the same jet or in the back-to-back jets. Jet pairs were simulated using minimum bias events generated with PYTHIA[6] with the branching ratio of the π^0 Dalitz decay set to 100% to enhance the sample of jet pairs per event. We exclude all pairs from single hadron decays so that cross pairs as well as any signal in the unlike-sign pairs are removed. Electrons and positrons from cross and jet pairs are filtered through the PHENIX acceptance and weighted according to the electron identification and ERT trigger efficiency. Pairs from simulated mixed events are subtracted from the like- and unlike-sign pair distributions to find the correlated pair distributions. The mixed event background is normalized by the same method used in the data analysis, described previously. It was found that correlated pairs from the same jet typically have small mass and large p_T while those from back-to-back jets have large mass and smaller p_T.

Correlated background pairs occur in all charge combinations. The simulated correlated like-sign background is then normalized to the measured correlated like-sign background by simultaneously fitting simulated cross and jet pair mass distributions to the measured correlated like-sign pair mass spectrum. Since the Monte Carlo simulation preserves the relative abundance of like- and unlike-sign pairs after filtering them through the

[5] The PHENIX acceptance is parameterized as function of the azimuthal angle ϕ of a track, its p_T, and charge sign q by conditions for the DC and the RICH for each spectrometer arm separately: $\phi_{\min} < \phi + qk_{\rm DC}/p_T < \phi_{\max}$ and $\phi_{\min} < \phi + qk_{\rm RICH}/p_T < \phi_{\max}$. The parameters are $k_{\rm DC} = 0.206$ rad GeV c^{-1}, $k_{\rm RICH} = 0.309$ rad GeV c^{-1}, $\phi_{\min} = -3/16\pi$ to $\phi_{\max} = 5/16\pi$, and $\phi_{\min} = 11/16\pi$ to $\phi_{\max} = 19/16\pi$.

[6] We used PYTHIA 6.319 changing PYTHIA parameters as follows: MSEL = 0 with the following processes switched on MSUB 11, 12, 13, 28, 53, 68, PARP(91) = 1.5 (k_T), MSTP(32) = 4 (Q^2 scale), and CKIN(3) = 2.0 (min. parton p_T).

PHENIX acceptance, we apply the same two normalization factors, one for cross- the other for jet-pairs, to the unlike-sign correlated background. The normalized contributions of both correlated background sources are also shown in Fig. 1. The unlike-sign dilepton signal is extracted by subtracting the simulated unlike-sign correlated backgrounds from the distribution of all correlated pairs.

In our second method to estimate the unlike-sign pair background we make no assumptions about the shape of the correlated background nor about the decomposition of correlated and uncorrelated background (see pp. 85–86 in [13]). We use the measured like-sign distribution which contains only the background, but with a different acceptance than the unlike-sign. We correct for this acceptance difference with the ratio of the mixed event distributions, $N_{+-}/2\sqrt{N_{++}N_{--}}$ as a function of mass and p_T. Projected onto the mass axis the relative acceptance can be estimated by dividing the mixed event background shown in Fig. 1. Since the acceptance for pairs is a function of mass and p_T, we have checked that for different e^+e^- pair sources, which span reasonable variations in mass and p_T shapes of the e^+e^- pairs, the relative acceptance is unchanged. The corrected like-sign distribution is then subtracted from the unlike-sign pairs without further normalization. Up to 3.5 GeV/c^2 the difference between the signal extracted using the two background subtraction techniques agrees to better than ±10%. Above 3.5 GeV/c the difference becomes much larger, which may indicate additional correlated background. In this region we subtract the measured like-sign yield, the larger of our two background estimates, and include the difference of the two methods as asymmetric systematic uncertainty on the signal yield.

In the next step the signal is corrected for electron reconstruction efficiency and trigger efficiency. The electron reconstruction efficiency was determined with a Monte Carlo simulation of the PHENIX detector (similar to [12]). The trigger efficiency for single electrons was measured using the MB sample. For each of the 8 calorimeter sectors we determine the ratio of electrons that fired the ERT trigger to all electrons reconstructed as function of p_T. Pairs from hadron decays simulated with EXODUS are filtered by the acceptance and then folded with the ERT trigger efficiency to extract the pair trigger efficiency as function of mass. At high masses the trigger efficiency saturates at 72%, limited by the active area of the trigger, from 1.5 to 0.5 GeV/c^2 the pair efficiency gradually drops to 32% and remains approximately constant at lower masses. In addition, the yield is divided by $0.79/0.55 = 1.44$ to account for the fraction of the inelastic $p+p$ cross section missed by our interaction trigger. The systematic uncertainties on the fully corrected spectrum shown in Fig. 2 are summarized in Table 1.

We model the e^+e^- pair contributions from hadron decays using the EXODUS decay generator. We follow closely the approach given in [5,14], however, we have updated all input to match the most recent PHENIX data. We assume that all hadrons have a constant rapidity density in the range $|\Delta\eta| \leqslant 0.35$ and a homogeneous distribution in azimuthal angle. Transverse momentum distributions are based on measurements in the same experiment where possible. The key input is the rapidity density $dN/dy = 1.06 \pm 0.11$ of neutral pions, which we determine from a fit to PHENIX data on charged and neutral pions, as shown in Fig. 3. The functional form of the pion transverse momentum distribution is given by:

$$E\frac{d^3\sigma}{dp^3} = A\left(e^{-(ap_T+bp_T^2)} + p_T/p_0\right)^{-n} \quad (1)$$

with $A = 377 \pm 60$ mb GeV$^{-2}\,c^3$, $a = 0.356 \pm 0.014$ (GeV/c)$^{-1}$, $b = 0.068 \pm 0.019$ (GeV/c)$^{-2}$, $p_0 = 0.7 \pm 0.02$ GeV/c and the power $n = 8.25 \pm 0.04$. For all other mesons we assume m_T scaling, replacing p_T by $\sqrt{m^2 - m_\pi^2 + (p_T/c)^2}$, where m is the mass of the meson. For the η, ω, ϕ, and J/ψ we fit a normalization factor to PHENIX data. In Fig. 3 the results are compared to published PHENIX data; excellent agreement with the data is achieved. The η meson is measured only at higher p_T, however, the fit is in good agreement with the p_T distribution of kaons, which have similar mass.

In order to extract the meson yield per inelastic $p+p$ collision we integrate the fits over all p_T. Results, systematic uncertainties, and references to data are given in Table 2. For the ρ meson we assume $\sigma_\rho/\sigma_\omega = 1.15 \pm 0.15$, consistent with values found in jet fragmentation [15]. The η' yield is scaled to be consistent with jet fragmentation $\sigma_{\eta'}/\sigma_\eta = 0.15 \pm 0.15$ [15]. The ψ' is adjusted to the value of $\sigma_{\psi'}/\sigma_{J/\psi} = 0.14 \pm 0.03$ [22]. For the η, ω, ϕ, and J/ψ the quoted uncertainties include those on the data as well as those using different shapes of the p_T distributions to extrapolate to zero p_T. Specifically we have fitted the functional form given in Eq. (1) with all parameters free and also an exponential distribution in m_T. For the ρ, η', and ψ' the uncertainty is given by the uncertainty we assumed for the cross section ratios. We note that the dilepton spectra from meson decays are rather insensitive to the exact shape of the p_T distribution.

Once the meson yields and p_T spectra are known the dilepton spectrum is given by decay kinematics and branching ratios, which are implemented in our decay generator EXODUS following earlier work published in [5,14]. The branching ratios are taken from the compilation of particle properties in [15]. For the Dalitz decays π^0, η, $\eta' \to e^+e^-\gamma$ and the decay $\omega \to e^+e^-\pi^0$ we use the Kroll–Wada expression [23] with electromagnetic transition form factors measured by the Lepton-G Collaboration [24,25]. For the decays of the vector mesons ρ, ω, $\phi \to e^+e^-$ we use the expression derived by Gounaris and Sakurai [26], extending it to 2 GeV/c^2, slightly beyond its validity range. For the J/ψ and $\psi' \to e^+e^-$ we use the same expression modified to include radiative corrections as discussed in [21]. All vector mesons are assumed to be unpolarized. The resulting dilepton spectra are compared to our data in Fig. 2 with the systematic uncertainties shown as a band. They are calculated as a function of mass and are dominated by the uncertainties on the meson yield tabulated in Table 2. The uncertainty from the measured electromagnetic transition form factors, in particular for the $\omega \to e^+e^-\pi^0$ decay, is also included but contributes visibly only in the range around 500 to 600 MeV/c^2. Also shown on Fig. 2 are the contributions from open charm and bottom production, discussed in more detail below, as well as from the Drell–Yan process, which is negligible. The bottom panel shows the ratio of data to the sum of all sources, hadronic cocktail, charm, bottom and Drell–Yan. The data agree very well with the sum of all known sources within the quoted systematic uncertainties.

Except for the vector meson peaks, the dilepton yield in the mass range above 1.1 GeV/c^2 is dominated by semileptonic decays of D and B mesons correlated through flavor conservation. To determine this contribution we subtract the meson decay cocktail from the dilepton data, the resulting mass spectrum is shown in Fig. 4. In the PHENIX acceptance the integrated e^+e^- pair yield per event from heavy flavor decays in the range from 1.1 to 2.5 GeV/c^2 is $4.21 \pm 0.28(\text{stat}) \pm 1.02(\text{syst}) \times 10^{-8}$. The systematic uncertainties are those tabulated in Table 1 plus the uncertainty on the cocktail subtraction. The cocktail subtraction is dominated by the high mass end of the broad ρ resonance. The ρ contribution in this region is not very well known and we therefore assume 100% systematic uncertainty on the ρ contribution. To estimate the rapidity density of $c\bar{c}$ pairs the measured e^+e^- pair yield is corrected for the geometrical acceptance, i.e., corrected from requiring both electron and positron within the PHENIX central arm acceptance to having the electron pair within one unit of rapidity at mid-rapidity. It then is extrapolated to zero e^+e^- pair mass and converted to $c\bar{c}$ using known branching ratios of semileptonic decays [15]. This

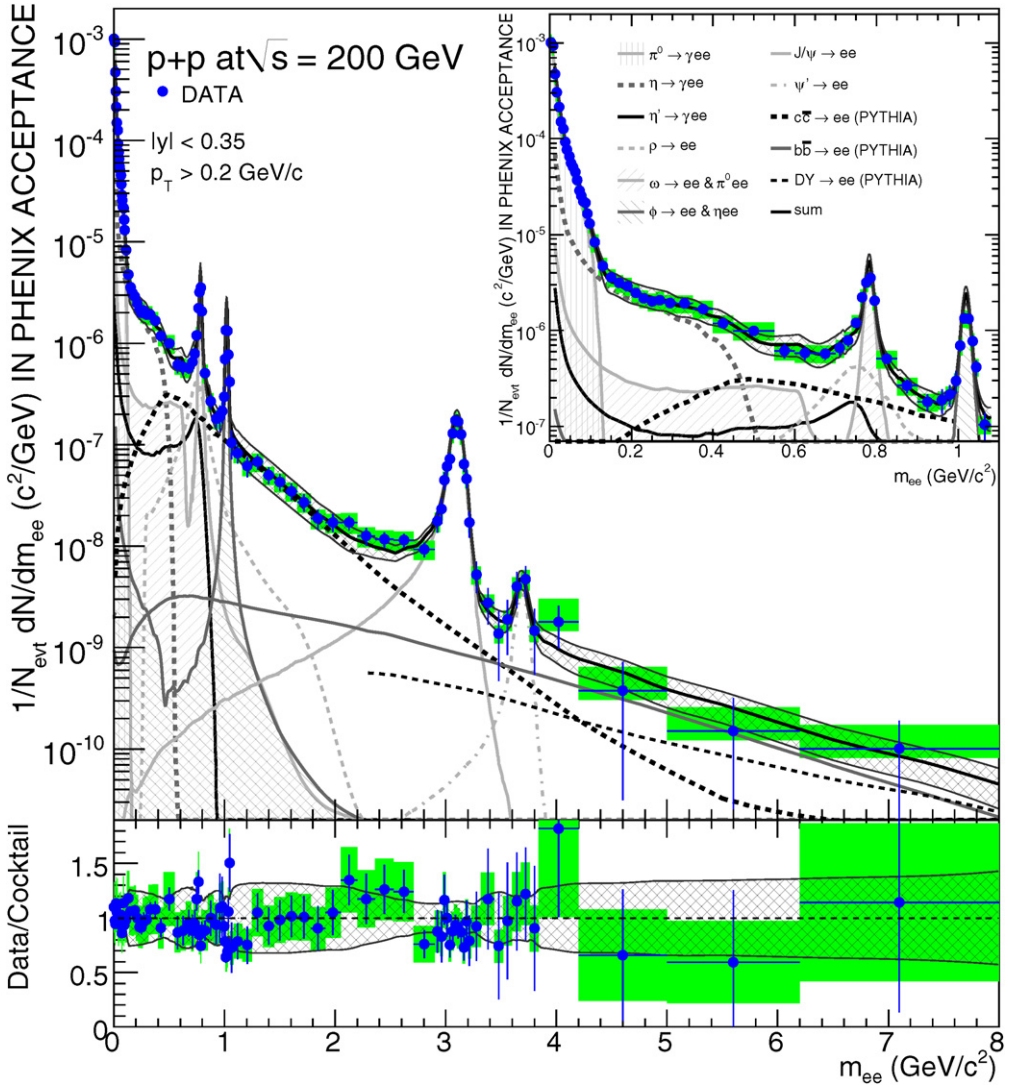

Fig. 2. Electron–positron pair yield per inelastic $p + p$ collision as function of pair mass. Data show statistical (bars) and systematic (shades) errors separately. The yield per event can be converted to a cross section by multiplying with the inelastic $p + p$ cross section of 42.2 mb. The data are compared to a cocktail of known sources. The contribution from hadron decays is independently normalized based on meson measurements in PHENIX, the systematic uncertainties are given by the error band. The contribution from open charm production is scaled to match the data ($\sigma_{c\bar{c}} = 544 \pm 39(\text{stat}) \pm 142(\text{syst}) \pm 200(\text{model})$ μb). The inset shows the same data but focuses on the low mass region. The bottom panel shows the ratio of data to the cocktail of known sources. The systematic uncertainties of the data are shown as boxes, while the uncertainty on the cocktail is shown as band around 1.

Table 1
Systematic uncertainties of the dilepton yield due to different sources and for different mass ranges. The uncertainties vary with mass and the largest uncertainties are quoted for each mass range. The contribution quoted for the jet pair subtraction also accounts for the difference in the signal observed between our two background subtraction techniques.

	< 0.4 GeV/c^2	0.4–1.1 GeV/c^2	1.1–3.5 GeV/c^2	> 3.5 GeV/c^2
Minimum bias trigger	11.3%	11.3%	11.3%	11.3%
ERT trigger efficiency	5%	5%	5%	5%
Conversion rejection	5%	–	–	–
Mixed event background	2%	8%	4%	–
Cross pair subtraction	$< 1\%$	–	–	–
Jet pair subtraction	2%	3%	11%	+70%
Reconstruction efficiency	14.4%	14.4%	14.4%	14.4%
Total	19.8%	20.8%	22.3%	+73%, −19%

correction is model dependent; we used our tuned PYTHIA simulation[7] to directly relate e^+e^- pairs from charm in the PHENIX acceptance and in the mass range from 1.1 to 2.5 GeV/c^2 to the $c\bar{c}$ rapidity density.[8]

[7] We used PYTHIA 6.205 with CTEQ5L parton distribution function [31]. We changed PYTHIA parameters as follows: PARP(91) = 1.5 (k_T), PARP(31) = 3.5 (K factor), MSTP(33) = 1, MSTP(32) = 4 (Q^2 scale) and in addition for charm production we use MSEL = 11 and PMAS(4, 1) = 1.25 (mass), for bottom MSEL = 5 and PMAS(5, 1) = 4.1 (mass), and for Drell–Yan MSEL = 11, PARP(31) = 1.8, and CKIN(3) = 2.0 (min. parton p_T).

[8] It is known that lowest order PYTHIA calculations, as we use, fail to describe single electron production from charmed quarks produced with large p_T. This is

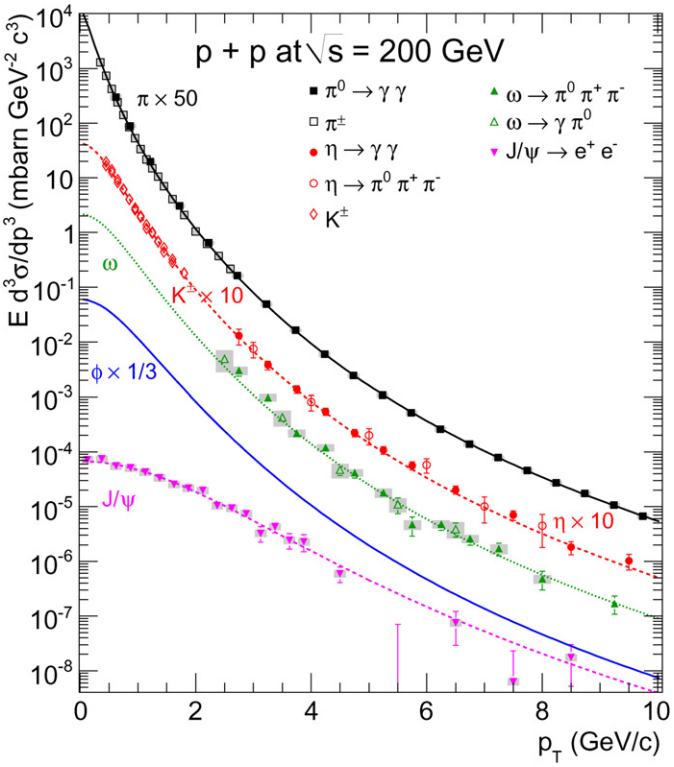

Fig. 3. Compilation of meson production cross sections in $p+p$ collisions at $\sqrt{s}=200$ GeV. Shown are data for neutral [16] and charged pions [17], η [18], kaons [17], ω [19], and J/ψ [21]. The data are compared to the parameterization based on m_T scaling of the measured pion distribution, as used in our hadron decay generator.

Table 2
Hadron rapidity densities used in our hadron decay generator. For the ω and ϕ meson data from this analysis were used together with data from the quoted references.

	$\frac{dN}{dy}\|_{y=0}$	Relative err.	Data used
π^0	1.065 ± 0.11	10%	PHENIX [16,17]
η	0.11 ± 0.03	30%	PHENIX [18]
ρ	0.089 ± 0.025	28%	jet fragmentation [15]
ω	0.078 ± 0.018	23%	PHENIX [19]
ϕ	0.009 ± 0.002	24%	PHENIX [20]
η'	0.016 ± 0.016	100%	jet fragmentation [15]
J/ψ	$(1.77 \pm 0.27) \times 10^{-5}$	15%	PHENIX [21]
ψ'	$(2.5 \pm 0.7) \times 10^{-6}$	27%	world average [22]

For single tracks the acceptance is known to better than 5%. Neglecting correlations between the electron and positron this implies an uncertainty of less than 10% for pairs. However, the fraction of e^+e^- pairs from correlated heavy flavor decays at mid-rapidity depends on the dynamical correlations between the quarks. These are not very accurately known [27], in particular in the azimuthal direction. Therefore additional systematic uncertainties need to be considered. In PYTHIA the intrinsic k_T parameter modifies the azimuthal correlation between c and $\bar{c}$. We have varied k_T between 1 and 3 GeV/c and reevaluate the fraction of e^+e^- pairs at mid-rapidity. A $\pm 20\%$ variation was found. Different choices of parton distribution functions (PDFs) lead to modifications of the longitudinal correlation of the pair, often expressed as the rapidity gap between the c and $\bar{c}$ quarks. We used different

not a concern for our analysis, since the majority of the e^+e^- pairs in our mass spectrum result from $c\bar{c}$ pairs where the c and $\bar{c}$ have low p_T and large opening angle. Future analysis of the pair p_T dependence, however, will need to take this into account.

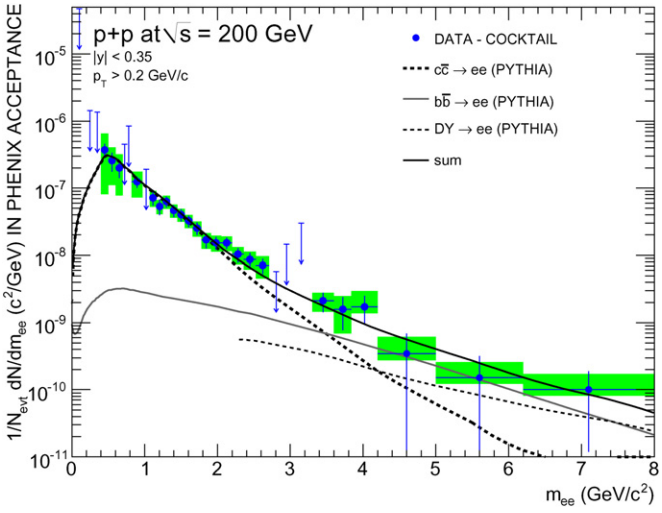

Fig. 4. Electron–positron mass distributions from semileptonic decays of heavy flavor, obtained by subtracting the contribution from π^0, η, ω, ρ, ϕ, η', J/ψ and ψ' mesons from the inclusive e^+e^- pair yield. The arrows indicate upper limits (95% CL) in the mass regions where the charm contribution is smaller or comparable to the systematic uncertainties. For all data points statistical error bars and systematic uncertainty boxes, including data and model contributions, are shown. Also shown is the contribution from charm ($\sigma_{c\bar{c}} = 544 \pm 39(\text{stat}) \pm 142(\text{syst}) \pm 200(\text{model})$ μb), as well as expected contributions from bottom ($\sigma_{b\bar{b}} = 3.7$ μb) and Drell–Yan ($\sigma_{b\bar{b}} = 0.04$ μb).

parton distribution functions available in PYTHIA, specifically we have used CTEQ5L, CTEQ4L, GRV94LO, GRV98LO, and MRST(c-g). We find $\pm 11\%$ deviations for the e^+e^- pair yield in the PHENIX acceptance. When converting the e^+e^- pair yield to $c\bar{c}$ pairs there is also a $\pm 21\%$ uncertainty resulting from uncertainties of relative abundance of charmed hadrons and of the branching ratios to semileptonic decays. We use an effective branching ratio for $c \to e$ of $9.5\% \pm 1\%$, which was calculated from $D^+/D^0 = 0.45 \pm 0.1$, $D_s/D^0 = 0.25 \pm 0.1$, and $\Lambda_c/D^0 = 0.1 \pm 0.05$ and the branching ratios from [15]. The overall uncertainty on the extrapolation is approximately 33%.

We also subtract a 7% contribution from bottom decays and the Drell–Yan mechanism for which we assign a 100% systematic uncertainty. For the bottom cross section we assume 3.7 μb [29], in agreement with our data above 4 GeV/c^2. Though negligible, we have also included the contribution from the Drell–Yan mechanism based on a cross section of 0.04 μb [28]. For the rapidity density of $c\bar{c}$ pairs at mid-rapidity we find:

$$\left.\frac{d\sigma_{c\bar{c}}}{dy}\right|_{y=0} = 118.1 \pm 8.4(\text{stat}) \pm 30.7(\text{syst}) \pm 39.5(\text{model})\ \mu\text{b}. \quad (2)$$

The systematic uncertainties on the data analysis and on the model dependent extrapolation are quoted separately. Using the rapidity distribution from HVQMNR [30] with CTEQ5M [31] PDF as in [5], the total charm cross section is $\sigma_{c\bar{c}} = 544 \pm 39(\text{stat}) \pm 142(\text{syst}) \pm 200(\text{model})$ μb. The extrapolation to 4π adds another 15% systematic uncertainty, which is included in the last term. The charm contribution as shown in Figs. 2 and 4 has been scaled to this result, which is compatible with our previous measurement of single electrons, which gave $\sigma_{c\bar{c}} = 567 \pm 57(\text{stat}) \pm 224(\text{syst})$ μb [5], and with the FONLL prediction of 256^{+400}_{-146} μb [3].

Instead of fixing the bottom cross section, we have tried an alternative approach. We take the shape of the bottom and charm e^+e^- pair distributions from PYTHIA filtered into the PHENIX acceptance and then fit the charm and bottom contribution to the data. For the charm cross section we obtain $\sigma_{c\bar{c}} = 518 \pm 47(\text{stat}) \pm 135(\text{syst}) \pm 190(\text{model})$ μb, consistent with our earlier analysis. The bottom cross section is $\sigma_{b\bar{b}} = 3.9 \pm 2.5(\text{stat})^{+3}_{-2}(\text{syst})$ μb. In addition

to the model dependent systematic uncertainties, which are similar to those on the charm extraction, the subtraction of e^+e^- pairs from the Drell–Yan mechanism contributes an extra 10–20% [32]. We estimate that the combined systematic uncertainty is about 50% and thus similar to the statistical error. The value for the bottom cross section is consistent with our earlier assumption of 3.7 μb as well as with the FONLL prediction of $1.87^{+0.99}_{-0.67}$ μb [3].

In conclusion, we have measured e^+e^- pairs in the mass range from 0 to 8 GeV/c^2 in $p+p$ collisions at $\sqrt{s}=200$ GeV. Within the systematic uncertainties the data can be described by known contributions from light meson decays, mostly measured in the same experiment, as well as from semileptonic decays of mesons carrying heavy flavor. The required charm and bottom production cross sections are consistent with the upper FONLL predictions and with the PHENIX measurement of single electrons.

Acknowledgements

We thank the staff of the Collider-Accelerator and Physics Departments at BNL for their vital contributions. We acknowledge support from the Department of Energy and NSF (USA), MEXT and JSPS (Japan), CNPq and FAPESP (Brazil), NSFC (China), IN2P3/CNRS, and CEA (France), BMBF, DAAD, and AvH (Germany), OTKA (Hungary), DAE (India), ISF (Israel), KRF and KOSEF (Korea), MES, RAS, and FAAE (Russia), VR and KAW (Sweden), US CRDF for the FSU, US–Hungarian NSF-OTKA-MTA, and US–Israel BSF.

References

[1] K. Adcox, et al., Nucl. Phys. A 757 (2005) 184.
[2] C. Aidala, et al., BNL-73798-2005 (2005); available at http://spin.riken.bnl.gov/rsc/report/masterspin.pdf.
[3] M. Cacciari, et al., Phys. Rev. Lett. 95 (2005) 122001.
[4] D. Acosta, et al., CDF Collaboration, Phys. Rev. Lett. 91 (2003) 241804.
[5] A. Adare, et al., PHENIX Collaboration, Phys. Rev. Lett. 97 (2006) 252002.
[6] S.S. Adler, et al., PHENIX Collaboration, Phys. Rev. D 76 (2007) 092002.
[7] R. Vogt, arXiv: 0709.2531 [hep-ph].
[8] B.I. Abelev, et al., STAR Collaboration, Phys. Rev. Lett. 98 (2007) 192301.
[9] J. Adams, et al., STAR Collaboration, Phys. Rev. Lett. 94 (2005) 062301.
[10] K. Adcox, et al., PHENIX Collaboration, Nucl. Instrum. Methods 499 (2003) 469.
[11] A. Toia, et al., PHENIX Collaboration, PoS CPOD07 (2007) 037.
[12] S. Afanasiev, et al., PHENIX Collaboration, arXiv: 0706.3034 [nucl-ex].
[13] T. Dahms, PhD Thesis (2008), Stony Brook University, arXiv: 0810.3040 [nucl-ex].
[14] G. Agakichiev, et al., CERES Collaboration, Eur. Phys. J. C 4 (1998) 231.
[15] W.M. Yao, et al., J. Phys. G 33 (2006) 1.
[16] A. Adare, et al., PHENIX Collaboration, Phys. Rev. D 76 (2007) 051106.
[17] S.S. Adler, et al., PHENIX Collaboration, Phys. Rev. C 74 (2006) 024904.
[18] S.S. Adler, et al., PHENIX Collaboration, Phys. Rev. C 75 (2007) 024909.
[19] S.S. Adler, et al., PHENIX Collaboration, Phys. Rev. C 75 (2007) 051902.
[20] Y. Riabov, et al., PHENIX Collaboration, J. Phys. G 34 (8) (2007) S925.
[21] A. Adare, et al., PHENIX Collaboration, Phys. Rev. Lett. 98 (2007) 232002.
[22] R. Gavai, et al., Int. J. Mod. Phys. A 10 (1995) 3043.
[23] N.M. Kroll, W. Wada, Phys. Rev. 98 (1955) 1355.
[24] R.I. Dzhelyadin, et al., Phys. Lett. B 102 (1981) 296.
[25] L.G. Landsberg, Phys. Rep. 128 (1985) 301.
[26] G.J. Gounaris, J.J. Sakurai, Phys. Rev. Lett. 21 (1968) 244.
[27] E.M. Aitala, et al., E791 Collaboration, Eur. Phys. J. C 1 (1999) 4.
[28] S. Gavin, et al., Int. J. Mod. Phys. A 10 (1995) 2961.
[29] C.H. Jaroschek, Masters Thesis (2001), Stony Brook University; the bottom cross section was obtained by tuning PYTHIA to experimental data and interpolating to $\sqrt{s}=200$ GeV.
[30] M.L. Mangano, P. Nason, G. Ridolfi, Nucl. Phys. B 405 (1993) 507.
[31] H.L. Lai, et al., Eur. Phys. J. C 12 (2000) 375.
[32] W. Vogelsang, private communication.